

Curie-like paramagnetism due to incomplete Zhang-Rice singlet formation in $\text{La}_{2-x}\text{Sr}_x\text{CuO}_4$ C. V. Kaiser,¹ W. Huang,^{1,*} S. Komiya,² N. E. Hussey,³ T. Adachi,⁴ Y. Tanabe,^{4,†} Y. Koike,⁴ and J. E. Sonier^{1,5}¹*Department of Physics, Simon Fraser University, Burnaby, British Columbia, Canada V5A 1S6*²*Central Research Institute of Electric Power Industry, Yokosuka, Kanagawa 240-0196, Japan*³*H. H. Wills Physics Laboratory, University of Bristol, Bristol BS8 1TL, United Kingdom*⁴*Department of Applied Physics, Graduate School of Engineering, Tohoku University, Sendai 980-8579, Japan*⁵*Canadian Institute for Advanced Research, 180 Dundas Street West, Toronto, Ontario, Canada M5G 1Z8*

(Received 11 June 2012; revised manuscript received 13 August 2012; published 29 August 2012)

In an effort to elucidate the origin of the Curie-like paramagnetism that is generic for heavily overdoped cuprates, we have performed high-transverse-field muon spin rotation (TF- μ SR) measurements of $\text{La}_{2-x}\text{Sr}_x\text{CuO}_4$ single crystals over the Sr content range $0.145 \leq x \leq 0.33$. We show that the x dependence of the previously observed field-induced broadening of the internal magnetic field distribution above the superconducting transition temperature T_c reflects the presence of two distinct contributions. One of these becomes less pronounced with increasing x and is attributed to diminishing antiferromagnetic correlations. The other grows with increasing x , but decreases above $x \sim 0.30$, and is associated with the Curie-like term in the bulk magnetic susceptibility χ . In contrast to the Curie-like term, however, this second contribution to the TF- μ SR linewidth extends back into the underdoped regime. Our findings imply a coexistence of antiferromagnetically correlated and paramagnetic moments, with the latter becoming dominant beyond $x \sim 0.185$. This suggests that the doped holes do not neutralize all Cu spins via the formation of Zhang-Rice singlets. Moreover, the paramagnetic component of the TF- μ SR linewidth is explained by holes progressively entering the Cu $3d_{x^2-y^2}$ orbital with doping.

DOI: [10.1103/PhysRevB.86.054522](https://doi.org/10.1103/PhysRevB.86.054522)

PACS number(s): 74.72.Gh, 74.25.Ha, 76.75.+i

I. INTRODUCTION

In the heavily overdoped regime of hole-doped cuprates, T_c decreases with increasing hole concentration p , the normal-state pseudogap vanishes, and a Curie-like temperature dependence of the normal-state bulk¹⁻¹⁰ and local¹¹⁻¹⁵ spin susceptibilities appears. In $\text{La}_{2-x}\text{Sr}_x\text{CuO}_4$ (LSCO) where $p = x$, Oda *et al.*³ reported a Curie-like term appearing in the bulk magnetic susceptibility χ at $x \sim 0.18$, becoming more pronounced with increasing x , but weakening beyond $x \sim 0.30$. They attributed the Curie-like contribution to localized moments that break Cooper pairs and drive down T_c . However, the origin of such localized moments has never been established, and more recently this has prompted alternative explanations for the Curie-like behavior of χ .¹⁶ While often attributed to magnetic impurities or oxygen-disorder-induced defects, the Curie-like susceptibility appears to be a universal property of heavily overdoped cuprates, which has persisted through significant improvements in sample quality. In fact Takagi *et al.*¹ demonstrated early on that oxygen vacancies are not directly responsible for the Curie-like behavior. Nuclear magnetic resonance (NMR) studies of overdoped $\text{Tl}_{1-x}\text{Pb}_x\text{Sr}_2\text{CaCu}_2\text{O}_7$ (Ref. 13) and $\text{Bi}_2\text{Sr}_2\text{CaCu}_2\text{O}_{8+\delta}$ (Ref. 15) indicate that the source is paramagnetic moments localized in the CuO_2 planes. Wakimoto *et al.*¹⁰ have proposed that beyond $x = 0.22$, where a Curie-like term appears in their measurements of χ , 1/4 of the overdoped Sr ions may create the paramagnetic moments either via direct substitution of Sr on the Cu sites, or, as a more plausible scenario, via addition of holes that enter the Cu $3d_{x^2-y^2}$ orbitals. In either case, some fraction of the localized Cu magnetic moments are neutralized, breaking up the local antiferromagnetic (AF) order and liberating free Cu spins.

There is some recent evidence for holes predominantly entering the Cu $3d$ orbitals from Compton scattering

measurements on a LSCO $x = 0.30$ sample.¹⁷ This is a drastic departure from the widely accepted view that the doped holes mainly enter the O $2p$ band, creating Zhang-Rice singlets comprised of a Cu $3d_{x^2-y^2}$ hole state hybridized with a coherent superposition of O $2p_{x,y}$ orbitals from the four surrounding O atoms.¹⁸ The formation of Zhang-Rice singlets justifies the use of an effective single-band Hubbard or t - J model for a satisfactory description of the low-energy physics of the cuprates, rather than a three-band model containing both the in-plane Cu $3d_{x^2-y^2}$ and the O $2p_{x,y}$ orbitals. Based on x-ray absorption spectroscopy measurements of LSCO and $\text{Tl}_2\text{Ba}_2\text{CuO}_{6+\delta}$, Peets *et al.*¹⁹ have proposed yet another scenario, whereby the doped holes in the O $2p_{x,y}$ orbitals cease to hybridize with the Cu $3d_{x^2-y^2}$ states beyond $p \sim 0.20$. This would result in a loss of the oxygen-mediated in-plane AF superexchange interaction between the localized Cu spins. However, this is incompatible with neutron scattering measurements on LSCO that show some remnants of AF correlations persisting to at least $x = 0.25$.²⁰ Hence it is likely that some degree of hybridization persists in LSCO beyond $x \sim 0.20$.

Here we report high-transverse-field muon spin rotation (TF- μ SR) measurements on LSCO single crystals. Previous measurements of this kind revealed a T -dependent heterogeneous field response extending far above T_c .²¹⁻²⁵ Through a systematic study of the width of the internal magnetic field distribution above T_c as a function of Sr content x , MacDougall *et al.*²⁵ concluded that the most likely source of the heterogeneous line broadening is regions of staggered magnetization about the dopant Sr ions. In the present study we show that the T -dependent line broadening is associated with the Curie-like term in the bulk magnetic susceptibility. Consequently, a universal explanation is necessary to explain the similar p -dependent Curie term in χ for $\text{Tl}_2\text{Ba}_2\text{CuO}_{6+\delta}$,⁴

which is hole doped by increasing the oxygen content δ . In contrast to bulk magnetic susceptibility studies of LSCO, we make no assumptions about the T -dependent AF component to isolate the contribution of the localized paramagnetic moments. As a consequence, we find that the localized moments responsible for the Curie-like behavior of χ in heavily overdoped samples of LSCO also exist at lower hole doping—gradually becoming more pronounced with increasing x . We attribute the lack of a Curie-like term in χ below $x \sim 0.18$ to limitations of the assumed scaling function introduced by Johnston²⁶ to account for the AF correlations, and associate the paramagnetic moments with doped holes entering the Cu $3d_{x^2-y^2}$ orbital.

II. EXPERIMENTAL DETAILS

A. Samples

The LSCO single crystals studied here were cut from traveling-solvent floating-zone growth rods and subsequently annealed at elevated temperature and under oxygen partial pressure to minimize oxygen defects. The crystals were prepared by three different groups as follows: (i) Single LSCO crystals of Sr content $x = 0.145, 0.15, 0.166, 0.176, 0.19, 0.196, 0.216,$ and 0.24 with $T_c = 37.3, 37.6, 37.3, 37.1, 31.4, 30.5, 28,$ and 17 K, respectively, were grown by S. Komiya. These crystals were annealed at 800 to 900°C under low oxygen partial pressure (0.2 to 3.5 atm) for 200 h. Measurements were also performed on an as-grown $x = 0.19$ single crystal prepared by S. Komiya, which has a substantially reduced and very broad superconducting transition temperature of $T_c = 23 \pm 5$ K. The $x = 0.15, 0.166, 0.216,$ and 0.24 crystals were studied by zero-field (ZF) μSR in Refs. 27 and 28, and TF- μSR measurements of the $x = 0.166$ and 0.176 crystals were reported in Refs. 24 and 29. (ii) Six LSCO single crystals with $x = 0.26$ and $T_c = 12 \pm 2$ K, and two single crystals with $x = 0.30$ were synthesized by T. Adachi and Y. Tanabe. The $x = 0.26$ crystals were oxygen annealed at 1 atm and 900°C for 50 h, and subsequently slow cooled and kept at 500°C for 50 h. From chemical titration, the oxygen defect δ (defined as $\text{La}_{2-x}\text{Sr}_x\text{CuO}_{4-\delta}$) is estimated to be 0.014 ± 0.01 . The $x = 0.30$ crystals were oxygen annealed at 3 atm and 900°C for 100 h. Although we have not estimated δ for the $x = 0.30$ crystals, empirically we believe it is similar to that for the $x = 0.26$ sample. We note that bulk magnetic susceptibility measurements reveal superconducting diamagnetism in a tiny volume fraction of the $x = 0.30$ crystals below $T_c \sim 25$ K. (iii) Two LSCO single crystals with $x = 0.33$ were supplied by N. E. Hussey. One of these was a 380 mg as-grown crystal. Bulk magnetic susceptibility measurements of this crystal down to 2 K show no signs of superconductivity. The other 33.7 mg single crystal was annealed for two weeks under an extreme oxygen partial pressure of 400 atm at 900°C to minimize oxygen deficiencies and to ensure good homogeneity. Resistivity measurements show that this crystal exhibits no trace of superconductivity down to 0.1 K, but rather displays a T^2 resistivity,²⁷ which is a hallmark of a nonsuperconducting crystal. We note that superconducting inclusions would contribute a T -linear component to the resistivity.³⁰ The lack of any T -linear

component is good evidence of a relatively homogeneous nonsuperconducting sample with negligible phase separation. Low-temperature ZF- μSR measurements on this crystal have revealed a spin-freezing transition of unknown origin at 0.9 K.²⁷

B. Muon spin rotation

The TF- μSR experiments were carried out at TRIUMF in Vancouver, Canada, using the HiTime spectrometer, which consists of an ultralow-background sample holder contained inside a helium-gas-flow cryostat and a horizontal warm-bore 7 T superconducting magnet. Measurements at temperatures above $T \sim 2$ K were performed with an external magnetic field applied perpendicular to the direction of the initial muon spin polarization $\mathbf{P}(0)$, and parallel to the c axis ($\parallel \mathbf{c}$) of the LSCO crystals. The TF- μSR spectra for each sample are well described by the sum of a small time-independent background component from muons that miss the sample and evade the background suppression system, and the following power-exponential depolarization function:

$$P_i(t) = e^{-(\Lambda t)^\beta} \cos(\gamma_\mu B t + \phi_i), \quad (1)$$

where B is the magnitude of the average local magnetic field sensed by muons stopping in the sample, and ϕ_i is the phase angle between $\mathbf{P}(0)$ and the axis of the i th positron detector ($i = 1, 2, 3,$ and 4). The power exponential describes the relaxation of the TF- μSR signal, which occurs when there is a distribution of internal magnetic field. For static fields, a larger relaxation rate Λ signifies a broader field distribution, often referred to as inhomogeneous line broadening. If the local magnetic field sensed by each muon also fluctuates during its lifetime, motional narrowing of the linewidth occurs, such that Λ is reduced with increasing fluctuation rate. It is generally not possible to distinguish between static and dynamic depolarization of the TF- μSR signal.

III. RESULTS

A. Field-induced broadening

Figure 1 shows representative results of fits of the $x = 0.15$ and $x = 0.24$ TF- μSR signals at $H = 7$ T to Eq. (1). The relaxation rate Λ for all samples exhibits a Curie-like temperature dependence above T_c indicative of paramagnetic moments. The saturated value $\beta \sim 1.8$ above $T \sim 150$ K [see Fig. 1(b)] indicates that the depolarization of the TF- μSR signal at these temperatures is dominated by the dipolar fields of the nuclear moments, whereas the fluctuation rate of the electronic moments becomes too fast to cause significant dynamic depolarization. Below T_c there is an additional depolarization associated with the static inhomogeneous line broadening by vortices, which may or may not form a highly ordered lattice. The vortex line broadening is proportional to λ_{ab}^{-2} , where λ_{ab} is the in-plane magnetic penetration depth.³¹ The effect of the high-oxygen-pressure postannealing on the temperature dependence of Λ at $x = 0.33$ is shown in Fig. 2. The difference between Λ in the as-grown and annealed crystals grows significantly with decreasing temperature. The higher values of Λ for the as-grown crystal are ascribed to a spatial distribution of hole doping caused by oxygen

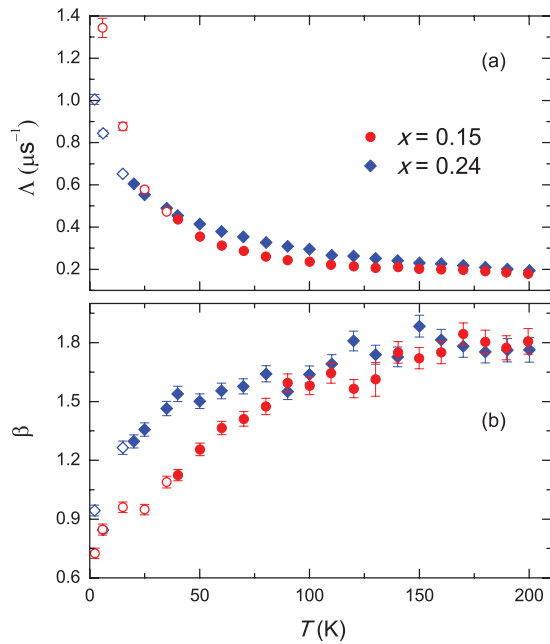


FIG. 1. (Color online) Temperature dependence of (a) the relaxation rate Δ , and (b) the power β from fits of the TF- μ SR signals of the $x = 0.15$ and $x = 0.24$ samples at $H = 7$ T to Eq. (1). The open symbols denote data at temperatures below T_c .

inhomogeneity, and, in particular, electronic moments from more underdoped regions of the sample.

Figure 3 shows the dependence of Δ on Sr concentration x at low temperatures. Below $x \sim 0.185$ the dependence of Δ on x is opposite to the hole-doping dependence of the zero-temperature extrapolated quantity $\lambda_{ab}^{-2}(0)$.^{32,33} This indicates that the width of the internal magnetic field distribution below $x \sim 0.185$ is not dominated by static vortices. While the decrease of Δ with increasing x could be caused by motional narrowing of the linewidth due to rapid fluctuations of the vortices on the μ SR time scale, Δ (and hence the linewidth)

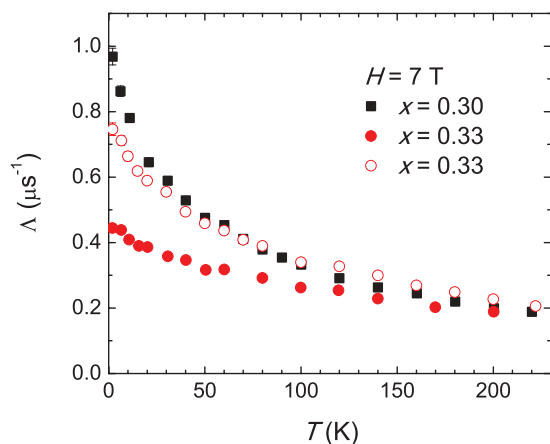


FIG. 2. (Color online) Comparison of the temperature dependence of the relaxation rate Δ at $H = 7$ T for the as-grown $x = 0.33$ single crystal (open red circles) and the $x = 0.33$ single crystal postannealed under high oxygen partial pressure (solid red circles). Also shown are data for the lower-pressure-annealed $x = 0.30$ sample.

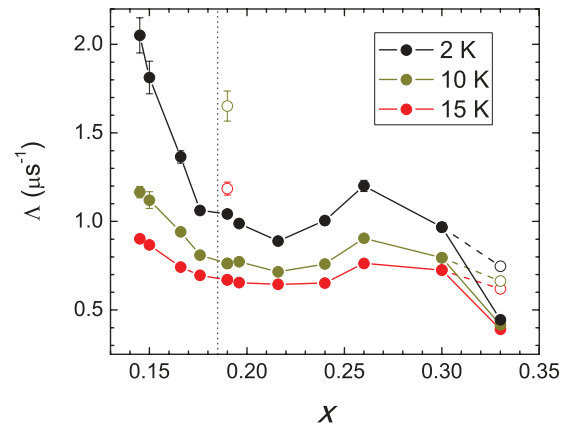


FIG. 3. (Color online) Dependence of Δ on Sr concentration x at $H = 7$ T for temperatures below T_c . The open circles are data for the as-grown $x = 0.19$ and $x = 0.33$ single crystals. The dashed vertical line indicates $x = 0.185$.

below T_c increases with increasing magnetic field,^{24,34} which is contrary to either a pure vortex-solid or vortex-liquid state. Neutron scattering measurements on LSCO at $H = 0$ show that remnant AF spin correlations of the parent insulator La_2CuO_4 vanish between $x = 0.25$ and $x = 0.30$.²⁰ At low temperatures the $H = 7$ T applied field appears to sufficiently stabilize the AF spin fluctuations, such that the temporal fluctuations of the local magnetic field sensed by the muon do not average to zero. Here we note that while elastic neutron diffraction experiments indicate that a field of $H \geq 13$ T is necessary to induce coexisting static AF order and superconductivity in $x \geq 0.145$ samples,³⁵ nonuniform static magnetism is observed in the vortex state by TF- μ SR at much lower fields.²⁹ The latter is explained by interlayer coupling that enables fluctuating magnetism to be stabilized by weakly interacting vortices.³⁶ With this said, the decrease of Δ with increasing x in Fig. 3 is explained by an increase in the Cu spin fluctuation rate, which reduces the dynamic depolarization of the TF- μ SR signal.

Just above $x \sim 0.185$, the near saturation of Δ in Fig. 3 indicates that the influence of the AF spin fluctuations on the TF- μ SR line width becomes negligible. Since measurements of $\lambda_{ab}^{-2}(0)$ in $0.07 \leq x \leq 0.24$ LSCO powders by Panagopoulos *et al.*³² show a saturation of $\lambda^{-2}(0)$ above $x = 0.19$, it appears that the TF- μ SR linewidth immediately above $x \sim 0.185$ is dominated by the static inhomogeneous field distribution of the vortex-solid phase. However, recent measurements of $0.06 \leq x \leq 0.30$ LSCO films by Lemberger *et al.*,³³ show $\lambda_{ab}^{-2}(0)$ decreasing with increasing x above $x = 0.19$, and vanishing at $x = 0.27$. The different x dependences of $\lambda_{ab}^{-2}(0)$ reported in Refs. 32 and 33 may be due to varying degrees of phase separation into superconducting and nonsuperconducting metallic regions—typical of heavily-overdoped LSCO,^{37–39} and other cuprates.⁴⁰ While the origin of this discrepancy is uncertain, the observed increase of Δ beyond $x \sim 0.216$ in Fig. 3 divulges another source of linewidth broadening superimposed on the effect of the vortices. Above the usual superconducting-to-nonsuperconducting phase transition at $x = 0.27$, the vortex contribution vanishes and the value of Δ shown in Fig. 3 is reduced. Note that while there is a trace amount of

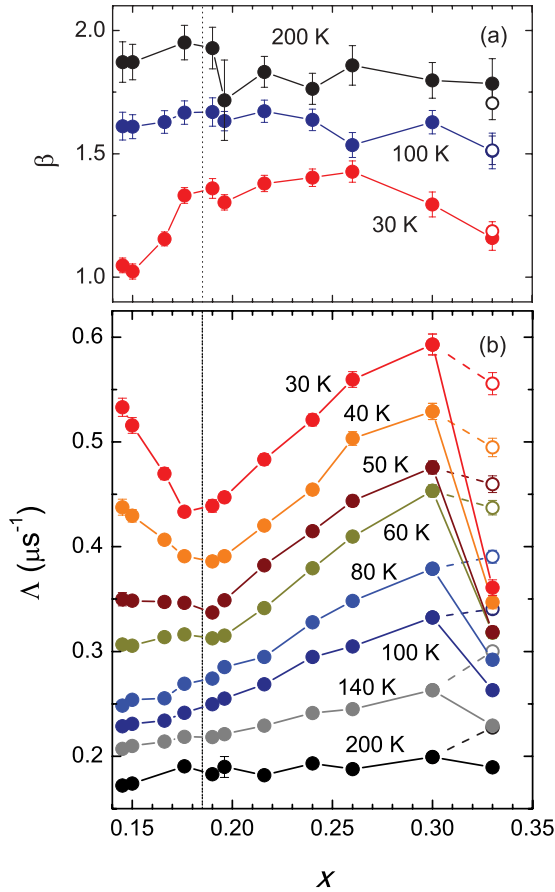


FIG. 4. (Color online) Dependence of (a) β and (b) Λ on Sr concentration x at $H = 7$ T and temperatures $T \geq 30$ K. The open circles are data for the as-grown $x = 0.33$ single crystal. The dashed vertical line indicates $x = 0.185$.

superconductivity in the $x = 0.30$ sample, the corresponding regions are likely not superconducting at $H = 7$ T.

Above T_c where the vortex contribution is absent, the component of Λ that increases with increasing x is more obvious and is seen to intensify up to $x = 0.30$ [see Fig. 4(b)]. At temperatures $T > 60$ K it becomes apparent that this component of Λ extends back to the lowest doping at $x = 0.145$. Hence it is clear that the source of this behavior is not restricted to heavily overdoped phase-separated samples, and does not onset at $x \sim 0.185$. Instead $x \sim 0.185$ appears to mark a low-temperature crossover from a hole-doping range where the dominant AF correlations to Λ comes from remnant AF correlations of the parent compound, to a higher hole-doping range dominated by a different kind and/or arrangement of magnetic moments. The slight increase of Λ with increasing x at $T = 200$ K in Fig. 4(b) implies that the line broadening at this temperature is dominated by the nuclear dipole moments. This conclusion is also reached from inspecting the corresponding values of β in Fig. 4(a). A complete summary of our measurements of Λ as a function of T and x is shown in Fig. 5.

B. Magnetic susceptibility and muon Knight shift

Figure 6(a) shows the temperature dependence of the bulk magnetic susceptibility of the annealed $x = 0.15$, $x = 0.24$,

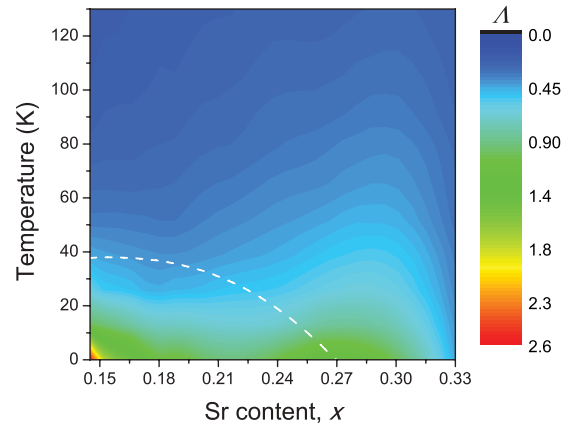


FIG. 5. (Color online) Contour plot of the variation of the relaxation rate Λ at $H = 7$ T with temperature and Sr content in the annealed LSCO single crystals. The phase diagram is generated by interpolating the Λ versus T data for each sample. The dashed white curve approximately indicates T_c at $H = 0$ T.

and $x = 0.33$ single crystals for $\mathbf{H} \parallel \mathbf{c}$. For $x > 0.08$ the magnetic susceptibility of LSCO in the normal state has previously been described by the following equation:

$$\chi(x, T) = \chi^{2D}(x, T) + \chi_0(x) + C(x)/T. \quad (2)$$

The contribution $\chi^{2D}(x, T)$ follows a simple universal scaling relation,²⁶ attributed to residual two-dimensional (2D) AF correlations in the CuO_2 planes. In particular, $\chi^{2D}(x, T)/\chi_{\text{max}}^{2D} = F(T/T_{\text{max}})$, where χ_{max}^{2D} and T_{max} are x -dependent values corresponding to the maximum of $\chi^{2D}(x, T)$ and F is a universal curve. The T -independent term $\chi_0(x)$ in Eq. (2) is

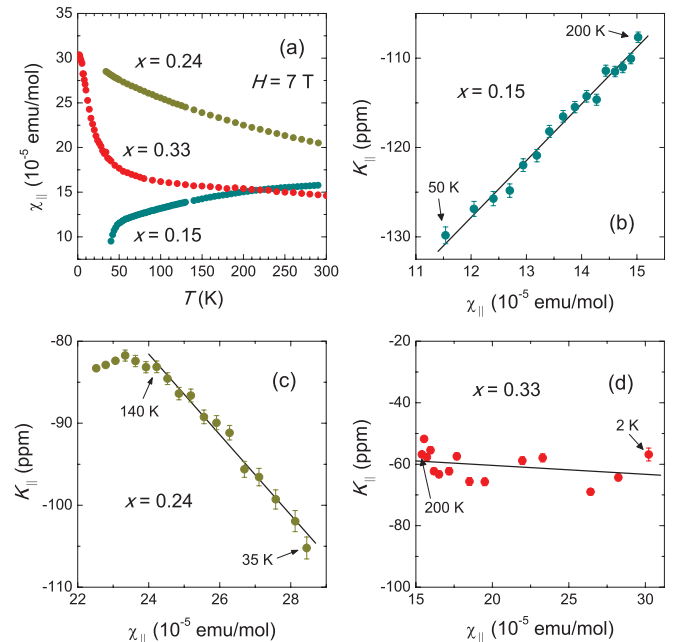


FIG. 6. (Color online) (a) Temperature dependence of the bulk molar susceptibility above T_c for a magnetic field $H = 7$ T applied parallel to the c axis. (b)–(d) Plots of the normal-state muon Knight shift versus the bulk molar susceptibility, with temperature as an implicit parameter.

the sum of the atomic core diamagnetism χ_{core} , the anisotropic Van Vleck paramagnetism χ_{VV} , and the Pauli paramagnetism χ_{Pauli} . As discussed later, the x dependence of χ_0 is caused by a variation of χ_{Pauli} . The third term in Eq. (2) has a Curie-like T dependence that appears above $x \sim 0.18$.^{3,6,10} The Curie constant $C(x)$ increases with increasing x above $x \sim 0.18$, signifying the growing presence of localized paramagnetic moments, but decreases beyond $x \sim 0.30$.

The local spin susceptibility causes a muon Knight shift, which is defined as the fractional difference between the average magnetic field B at the muon site and the applied field H . Correcting for macroscopic contributions to B that are present in the external field, the Knight shift originating from microscopic contributions in the sample is

$$K = \frac{B - H}{H} - K_{\text{dem},L}, \quad (3)$$

where $K_{\text{dem},L} = 4\pi(1/3 - N)\rho_{\text{mol}}\chi_{\parallel}$ is a correction for demagnetization and Lorentz fields, N is the demagnetization factor for the sample, ρ_{mol} is the molar density of the sample in units of mol/cm³, and χ_{\parallel} is the bulk molar susceptibility displayed in Fig. 6(a). The applied field induces spin polarization of both the conduction electrons and localized electronic moments, such that

$$K = K_0 + \frac{1}{H^2} \mathbf{H} \cdot \vec{A}_{\text{eff}} \cdot \vec{\chi} \cdot \mathbf{H}. \quad (4)$$

The first term is a T -independent contribution from the Pauli spin paramagnetism of the conduction electrons that screen the μ^+ charge. The second term is T dependent and arises from the polarization of localized electronic moments. It is expressed in terms of an effective hyperfine-coupling tensor \vec{A}_{eff} and the field-induced localized moment $\vec{\chi} \cdot \mathbf{H}$. The effective hyperfine coupling \vec{A}_{eff} is the sum of dipolar \vec{A}_{dip} and hyperfine contact coupling \vec{A}_{c} contributions. The elements of the dipolar coupling tensor \vec{A}_{dip} depend on the μ^+ site and the crystallographic structure, and are given by

$$A^{ij} = \sum_{\text{local}} \frac{1}{r^3} \left(3 \frac{r_i r_j}{r^2} - \delta_{ij} \right), \quad (5)$$

where the sum extends over all localized moments inside a Lorentz sphere, and r is the magnitude of the vector $\mathbf{r} = (x, y, z)$ connecting the muon site to the localized moment site in the crystal lattice. The hyperfine contact coupling, which is often considered as isotropic and T independent, results from further spin polarization of the conduction electrons by induced localized moments via the Rudermann-Kittel-Kasuya-Yosida (RKKY) interaction. In cuprates, an RKKY interaction may occur between localized Cu spins and doped itinerant holes. Calculations show that the RKKY interaction is enhanced with increasing hole concentration, and may dominate over the antiferromagnetic superexchange coupling in the overdoped regime.⁴¹⁻⁴³

Figures 6(b)–6(d) show the normal-state Knight shift (for $\mathbf{H} \parallel \mathbf{c}$) of the $x = 0.15$, $x = 0.24$, and $x = 0.33$ single crystals, corrected for demagnetization and Lorentz fields, and plotted versus χ_{\parallel} . For a wide range of temperature above T_c , K_{\parallel} exhibits linear scaling with χ_{\parallel} , indicating an equivalency of the bulk and local magnetic spin susceptibilities. The

saturation of K_{\parallel} at high temperatures for the $x = 0.24$ sample likely signifies the resolution limit of the measured TF- μ SR frequency shift. Likewise, the Knight shift at $x = 0.33$ appears to be too small to measure accurately with the spectrometer used in our experiments.

The most notable feature of the K_{\parallel} versus χ_{\parallel} plots is the change in the slope from positive at $x = 0.15$ to negative at $x = 0.24$. A positive slope was previously reported for $x = 0.07$.²³ The slope is equal to the effective hyperfine-coupling tensor element $A_{\text{eff}}^{\parallel}$ for $\mathbf{H} \parallel \mathbf{c}$. Unfortunately, the present measurements for a single direction of applied magnetic field are insufficient for determining the dipolar and contact hyperfine couplings. The problem is compounded by the apparent presence of both AF correlated spins and local paramagnetic moments. Consequently, to explain the changes in slope we resort to a heuristic argument. Recently it has been determined that the muon stops near the non-axially-symmetric site (0.120*a*, 0, 0.219*c*).²⁸ At this site and with $\mathbf{H} \parallel \mathbf{c}$, the calculated dipolar-coupling constant for antiferromagnetically ordered Cu spins (canted by 45° or lying in the *a-b* plane) is $A_{\text{dip}}^{\parallel} = -0.33$ kG/ μ_B . For parallel Cu spins aligned along the applied field direction, $A_{\text{dip}}^{\parallel} = 0.97$ kG/ μ_B . Hence the change in the sign of the slope between $x = 0.15$ and $x = 0.24$ can be explained by a change in the primary alignment of the Cu spins. However, the contact hyperfine-coupling constant A_{c}^{\parallel} is also expected to vary with x , not only because of a change in the effective exchange interaction between the Cu moment and the conduction electrons, but also, as discussed in the next section, because the density of electronic states at the Fermi energy is x dependent.

IV. DISCUSSION

We have shown that the normal state of LSCO single crystals from three different sources is characterized by a broad field-induced distribution of the internal magnetic field. The dependence of the TF- μ SR relaxation rate Λ on x indicates two distinct T -dependent contributions. The first of these decreases with increasing x and is clearly associated with diminishing remnant AF correlations. While neutron scattering^{20,44,45} and ZF- μ SR (Ref. 46) measurements on pure and Zn-doped LSCO in zero external magnetic field suggest that AF spin fluctuations likely persist out to the termination of superconductivity in the overdoped regime, the effect of AF correlations on the TF- μ SR line width at $H = 7$ T is apparent only up to $x \sim 0.185$. This is partly due to the diminishing effect of the applied magnetic field in stabilizing the increasingly faster AF fluctuations, but it is also a consequence of a second contribution to the TF- μ SR linewidth that grows with increasing x . We find, however, that this second source of line broadening is greatly reduced when superconductivity completely disappears beyond $x = 0.30$.

Since the Knight shift K_{\parallel} exhibits a linear scaling with χ_{\parallel} for a wide temperature range above T_c , it is instructive to consider the μ SR results in the context of comprehensive studies of the normal-state bulk magnetization of LSCO. To begin with, the T -independent component of the bulk magnetic susceptibility χ_0 is strongly dependent on the hole concentration. Measurements on samples in the range

$0.10 \leq x \leq 0.45$ show that χ_0 increases with increased hole doping, plateaus above $x \sim 0.20$ – 0.23 , and decreases above $x \sim 0.30$.^{6,47,48} While the T -independent component of the total static magnetic susceptibility includes contributions from the core diamagnetism and Van Vleck paramagnetism, the doping dependence of χ_0 has been attributed to changes in the Pauli susceptibility χ_{Pauli} . This is because the x dependences of χ_0 and the normal-state electronic specific heat coefficient γ are very similar below $x \sim 0.24$,⁴⁷ and in a free-electron system χ_{Pauli} and γ are each proportional to the density of states $N(E_F)$ at the Fermi energy. The x dependences of χ_{Pauli} and γ can be explained by the presence of a Van Hove singularity (VHS) in the electronic density of states caused by the flat part of the conduction bands of LSCO being very close to E_F . With increasing x , the $(\pi, 0)$ flatband and VHS move to higher energy and cross E_F at $x \sim 0.20$,^{49,50} where $N(E_F)$,⁵¹ and hence both χ_0 and γ reach their maximum values.

The increase of χ_0 with increasing x up to $x \sim 0.20$ is accompanied by a reduction of the effective moment of the localized Cu spins,^{6,47} due to the frustration effect of the doped holes in the O $2p_{x,y}$ orbitals on the AF exchange interaction between Cu spins. As mentioned above, the suppression of the AF correlations of the localized Cu spins is the source of the initial decrease of Λ with increasing x in Figs. 3, 4(b), and 5. On the other hand, we attribute the additional T -dependent contribution to Λ that grows with increasing x to the same source of the Curie-like constant $C(x)$ in the bulk magnetic susceptibility above $x \sim 0.18$. To see that this is the case, in Fig. 7 we compare $C(x)$ from Ref. 3 to $\Lambda(x)$ at $T = 80$ K, where the AF contribution is minor. Note that, as expected, the interpolated data of Ref. 3 fall between the two Λ values at $x = 0.33$, which correspond to the as-grown and high-oxygen-pressure-annealed extremes of sample preparation. While the $\Lambda(x)$ data points at $x = 0.33$ in Fig. 7 seem to suggest that the decrease of $C(x)$ beyond $x = 0.30$ is a sole consequence of the high-pressure anneal, the data at temperatures below $T = 80$ K in Fig. 4(b) clearly indicate that this is not the case.

In contrast to $C(x)$, the second T -dependent contribution to $\Lambda(x)$ extends below $x = 0.18$ into the underdoped regime.

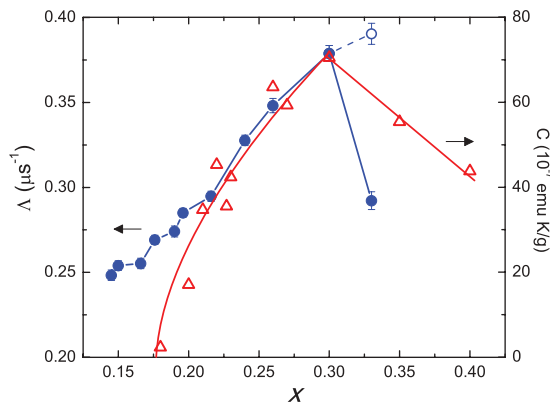


FIG. 7. (Color online) Comparison of the x dependence of Λ at $T = 80$ K to the x dependence of the Curie constant C from Ref. 3. The open circle corresponds to Λ for the as-grown $x = 0.33$ single crystal.

Strictly speaking, the Curie-like term observed in overdoped LSCO in Refs. 3 and 6 is the deviation of the bulk magnetic susceptibility from the assumed T -dependent form for $\chi^{2D}(x, T)$ in Eq. (2), which is described by the universal scaling function F introduced by Johnston.²⁶ Consequently, we ascribe the separation of the data for $C(x)$ and $\Lambda(x)$ below $x \sim 0.21$ in Fig. 7 to an inaccuracy in the assumed form for $\chi^{2D}(x, T)$. In actuality, Eq. (2) is valid only if the doped holes in the O $2p_{x,y}$ orbitals are weakly hybridized with the Cu $3d_{x^2-y^2}$ states,⁵ in which case $\chi_0(x)$ and $\chi^{2D}(x, T)$ can be treated as distinct terms. According to the x-ray absorption spectroscopy measurements by Peets *et al.*,¹⁹ this may be the case only at $x > 0.20$, where we find that the x dependence of Λ closely follows $C(x)$.

Electronic band calculations by Barbiellini and Jarlborg⁵² applied to the doping range $0.25 \leq x \leq 1$ show that weak ferromagnetic clusters are induced about concentrated regions of the Sr dopants in the heavily overdoped compound. Such ferromagnetic clusters have been offered as a potential source of the frozen moments observed in the annealed $x = 0.33$ single crystal below $T = 0.9$ K.²⁷ However, the calculated magnetic moment of the ferromagnetism grows with increasing x , which is at odds with the weakening of the Curie-like term and the decrease of Λ beyond $x = 0.30$.

Based on the following observations we conclude that the paramagnetic moments are the result of doped holes that do not stimulate the formation of Zhang-Rice singlets: (i) NMR measurements indicate that the source of the Curie-like paramagnetism resides in the CuO_2 layers, (ii) the Curie-like behavior is observed in cuprates hole doped by either cation substitution or changes in oxygen content, (iii) we find good agreement between samples synthesized by different groups, and (iv) we have demonstrated that the localized electronic moments responsible also exist in the underdoped regime.

Recently, Sordi *et al.* have shown that doublet formation (total spin $S = 1/2$) in a one-band Hubbard model grows upon doping the parent Mott insulator.⁵³ The same is true of the $S = 1/2$ three-spin polaron present in three-band models,^{54,55} where the spin of a hole on the in-plane oxygen is antiparallel to the two nearest-neighbor copper spins. However, the hole in these and the triplet state (total spin $S = 1$) is mobile, with the effective magnetic moment presumably fluctuating too fast to cause dynamic depolarization of the TF- μ SR signal.

The paramagnetic moments are more likely caused by a growing number of holes entering the Cu $3d$ orbitals, as evidenced by recent Compton scattering measurements of LSCO.¹⁷ Perry, Tahiri-Kheli, and Goddard⁵⁶ previously proposed that the doped holes in LSCO actually localize near the Sr dopant atoms in states that are an admixture of the out-of-plane Cu $3d_{z^2-r^2}$ and apical O $2p_z$ atomic orbitals. An analysis of neutron structural data in the range $0 \leq x \leq 0.375$ by Božin and Billinge⁵⁷ indicates that this is the case only for a small fraction of the doped holes, with this small percentage growing with increasing x . While charge doped into the apical bond may cause the out-of-plane Cu $3d_{z^2-r^2}$ orbital to carry a magnetic moment, this does not explain the reduction of C (and Λ) beyond $x \sim 0.30$. On the other hand, doped holes entering the half-filled in-plane Cu $3d_{x^2-y^2}$

orbital neutralize existing Cu spins, hence disrupting local AF order and creating free Cu spins. With doping, an increasing number of free Cu spins are generated in this way until the disappearance of AF correlations in the overdoped regime. The additional holes introduced by further doping progressively neutralizes the free Cu $3d_{x^2-y^2}$ spins, in agreement with the reduction of the Curie-like paramagnetism beyond $x \sim 0.30$. This appears to be a universal property of the cuprates, and consequently is a restriction on the applicability of one-band models.

ACKNOWLEDGMENTS

We thank G. A. Sawatzky and A.-M. S. Tremblay for informative discussions. We are also grateful to Z. Lotfi Mahyari, N. Mangkorntong, and the facility personnel at the TRIUMF Centre for Molecular and Materials Science for technical assistance. This work was supported by the Natural Sciences and Engineering Research Council of Canada, and the Canadian Institute for Advanced Research. N.E.H. acknowledges the support of a Royal Society Wolfson Research Merit Award.

*Present address: Department of Physics and Astronomy, McMaster University, Hamilton, Ontario, Canada L8S 4M1.

†Present address: Advanced Institutes for Materials Research (WPI-AIMR), Tohoku University, Sendai 980-8578, Japan.

¹H. Takagi, T. Ido, S. Ishibashi, M. Uota, S. Uchida, and Y. Tokura, *Phys. Rev. B* **40**, 2254 (1989).

²J. B. Torrance, A. Bezing, A. I. Nazzari, T. C. Huang, S. S. P. Parkin, D. T. Keane, S. J. LaPlaca, P. M. Horn, and G. A. Held, *Phys. Rev. B* **40**, 8872 (1989).

³M. Oda, T. Nakano, Y. Kamada, and M. Ido, *Physica C* **183**, 234 (1991).

⁴Y. Kubo, Y. Shimakawa, T. Manako, and H. Igarashi, *Phys. Rev. B* **43**, 7875 (1991).

⁵C. Allgeier and J. S. Schilling, *Phys. Rev. B* **48**, 9747 (1993).

⁶T. Nakano, M. Oda, C. Manabe, N. Momono, Y. Miura, and M. Ido, *Phys. Rev. B* **49**, 16000 (1994).

⁷G. A. Levin and K. F. Quader, *Physica C* **258**, 261 (1996).

⁸F. Schegolev, N. N. Kolesnikov, V. N. Kopylov, T. G. Togonidze, and O. M. Vyaselev, *J. Phys. I* **6**, 2265 (1996).

⁹G. Le Bras, Z. Konstantinovic, D. Colson, A. Forget, J.-P. Carton, C. Ayache, F. Jean, G. Collin, and Y. Dumont, *Phys. Rev. B* **66**, 174517 (2002).

¹⁰S. Wakimoto, R. J. Birgeneau, A. Kagedan, H. Kim, I. Swainson, K. Yamada, and H. Zhang, *Phys. Rev. B* **72**, 064521 (2005).

¹¹G.-Q. Zheng, T. Kuse, Y. Kitaoka, K. Ishida, S. Ohsugi, K. Asayama, and Y. Yamada, *Physica C* **208**, 339 (1993).

¹²L. Le Noc, A. Trokiner, J. Schneck, A. M. Pougnet, D. Morin, H. Savary, A. Yakubovskii, K. N. Mykhalyov, and S. V. Verkhovskii, *Physica C* **235–240**, 1703 (1994).

¹³P. V. Bellot, A. Trokiner, A. Yakubovskii, and L. Shustov, *Physica C* **282**, 1359 (1997).

¹⁴G. V. M. Williams, J. L. Tallon, R. Michalak, and R. Dupree, *Phys. Rev. B* **57**, 8696 (1998).

¹⁵B. Chen, S. Mukhopadhyay, W. P. Halperin, P. Guptasarma, and D. G. Hinks, *Phys. Rev. B* **77**, 052508 (2008).

¹⁶A. Kopp, A. Ghosal, and S. Chakravarty, *Proc. Natl. Acad. Sci. USA* **104**, 6123 (2007).

¹⁷Y. Sakurai, M. Itou, B. Barbiellini, P. E. Mijnders, R. S. Markiewicz, S. Kaprzyk, J.-M. Gillet, S. Wakimoto, M. Fujita, S. Basak, Y. J. Wang, W. Al-Sawai, H. Lin, A. Bansil, and K. Yamada, *Science* **332**, 698 (2011).

¹⁸F. C. Zhang and T. M. Rice, *Phys. Rev. B* **37**, 3759 (1988).

¹⁹D. C. Peets, D. G. Hawthorn, K. M. Shen, Y.-J. Kim, D. S. Ellis, H. Zhang, S. Komiyama, Y. Ando, G. A. Sawatzky, R. Liang, D. A. Bonn, and W. N. Hardy, *Phys. Rev. Lett.* **103**, 087402 (2009).

²⁰S. Wakimoto, K. Yamada, J. M. Tranquada, C. D. Frost, R. J. Birgeneau, and H. Zhang, *Phys. Rev. Lett.* **98**, 247003 (2007).

²¹A. T. Savici, A. Fukaya, I. M. Gat-Malureanu, T. Ito, P. L. Russo, Y. J. Uemura, C. R. Wiebe, P. P. Kyriakou, G. J. MacDougall, M. T. Rovers, G. M. Luke, K. M. Kojima, M. Goto, S. Uchida, R. Kadono, K. Yamada, S. Tajima, T. Masui, H. Eisaki, N. Kaneko, M. Greven, and G. D. Gu, *Phys. Rev. Lett.* **95**, 157001 (2005).

²²G. J. MacDougall, R. J. Birgeneau, H. Kim, S.-J. Kim, J. Rodriguez, P. L. Russo, A. T. Savici, Y. J. Uemura, S. Wakimoto, C. R. Wiebe, and G. M. Luke, *Physica B* **374–375**, 211 (2006).

²³K. Ishida, W. Higemoto, K. Ohishi, A. Koda, K. H. Satoh, R. Kadono, M. Fujita, and K. Yamada, *J. Magn. Magn. Mater.* **310**, 526 (2007).

²⁴J. E. Sonier, M. Ilton, V. Pacradouni, C. V. Kaiser, S. A. Sabok-Sayr, Y. Ando, S. Komiyama, W. N. Hardy, D. A. Bonn, R. Liang, and W. A. Atkinson, *Phys. Rev. Lett.* **101**, 117001 (2008).

²⁵G. J. MacDougall, A. T. Savici, A. A. Aczel, R. J. Birgeneau, H. Kim, S.-J. Kim, T. Ito, J. A. Rodriguez, P. L. Russo, Y. J. Uemura, S. Wakimoto, C. R. Wiebe, and G. M. Luke, *Phys. Rev. B* **81**, 014508 (2010).

²⁶D. C. Johnston, *Phys. Rev. Lett.* **62**, 957 (1989).

²⁷J. E. Sonier, C. V. Kaiser, V. Pacradouni, S. A. Sabok-Sayr, C. Cochran, D. E. MacLaughlin, S. Komiyama, and N. E. Hussey, *Proc. Natl. Acad. Sci. USA* **107**, 17131 (2010).

²⁸W. Huang, V. Pacradouni, M. P. Kennett, S. Komiyama, and J. E. Sonier, *Phys. Rev. B* **85**, 104527 (2012).

²⁹J. E. Sonier, F. D. Callaghan, Y. Ando, R. F. Kiefl, J. H. Brewer, C. V. Kaiser, V. Pacradouni, S. A. Sabok-Sayr, X. F. Sun, S. Komiyama, W. N. Hardy, D. A. Bonn, and R. Liang, *Phys. Rev. B* **76**, 064522 (2007).

³⁰N. E. Hussey, R. A. Cooper, Xiaofeng Xu, Y. Wang, I. Mouzopoulou, B. Vignolle, and C. Proust, *Philos. Trans. R. Soc. A* **369**, 1626 (2011).

³¹J. E. Sonier, R. F. Kiefl, and J. H. Brewer, *Rev. Mod. Phys.* **72**, 769 (2000).

³²C. Panagopoulos, T. Xiang, W. Anukool, J. R. Cooper, Y. S. Wang, and C. W. Chu, *Phys. Rev. B* **67**, 220502 (2003).

³³T. R. Lemberger, I. Hetel, A. Tsukada, M. Naito, and M. Randeria, *Phys. Rev. B* **83**, 140507(R) (2011).

³⁴J. E. Sonier, *J. Phys.: Condens. Matter* **22**, 203202 (2010).

³⁵J. Chang, Ch. Niedermayer, R. Gilardi, N. B. Christensen, H. M. Rønnow, D. F. McMorrow, M. Ay, J. Stahn, O. Sobolev, A. Hiess, S. Pailhes, C. Baines, N. Momono, M. Oda, M. Ido, and J. Mesot, *Phys. Rev. B* **78**, 104525 (2008).

- ³⁶S. A. Kivelson, D.-H. Lee, E. Fradkin, and V. Oganesyan, *Phys. Rev. B* **66**, 144516 (2002).
- ³⁷Y. Tanabe, T. Adachi, T. Noji, and Y. Koike, *J. Phys. Soc. Jpn.* **74**, 2893 (2005).
- ³⁸Y. Wang, J. Yan, L. Shan, H.-H. Wen, Y. Tanabe, T. Adachi, and Y. Koike, *Phys. Rev. B* **76**, 064512 (2007).
- ³⁹T. Adachi, S. M. Haidar, T. Kawamata, N. Sugawara, N. Kaneko, M. Uesaka, H. Sato, Y. Tanabe, T. Noji, K. Kudo, N. Kobayashi, and Y. Koike, in Proceedings of the 25th International Conference on Low Temperature Physics (LT25) [*J. Phys.: Conf. Ser.* **150**, 052115 (2009)].
- ⁴⁰H. H. Wen, S. L. Li, Z. W. Zhao, Z. Y. Liu, H. P. Yang, D. N. Zheng, and Z. X. Zhao, *Europhys. Lett.* **57**, 260 (2002).
- ⁴¹Q. Si, J. P. Lu, and K. Levin, *Phys. Rev. B* **45**, 4930 (1992).
- ⁴²J. J. Rodríguez-Núñez, H. Beck, J. Konior, A. M. Olés, and B. Coqblin, *Phys. Lett. A* **197**, 173 (1995).
- ⁴³E. Kolley, W. Kolley, and R. Tietz, *J. Phys.: Condens. Matter* **10**, 657 (1998).
- ⁴⁴O. J. Lipscombe, S. M. Hayden, B. Vignolle, D. F. McMorrow, and T. G. Perring, *Phys. Rev. Lett.* **99**, 067002 (2007).
- ⁴⁵S. D. Wilson, Z. Yamani, C. Dhital, B. Freelon, P. G. Freeman, J. A. Fernandez-Baca, K. Yamada, S. Wakimoto, W. J. L. Buyers, and R. J. Birgeneau, *Phys. Rev. B* **85**, 014507 (2012).
- ⁴⁶Risdiana, T. Adachi, N. Oki, S. Yairi, Y. Tanabe, K. Omori, Y. Koike, T. Suzuki, I. Watanabe, A. Koda, and W. Higemoto, *Phys. Rev. B* **77**, 054516 (2008).
- ⁴⁷T. Nakano, K. Yamaya, N. Momono, M. Oda, and M. Ido, *J. Low Temp. Phys.* **105**, 395 (1996).
- ⁴⁸J. W. Loram, K. A. Mirza, J. R. Cooper, N. Athanassopoulou, and W. Y. Liang, in *Proceedings of the Tenth Anniversary HTS Workshop of Physics, Materials and Applications*, edited by B. Batlogg, C. W. Chu, D. U. Gubser, and K. A. Müller (World Scientific, Singapore, 1996).
- ⁴⁹A. Ino, C. Kim, M. Nakamura, T. Yoshida, T. Mizokawa, A. Fujimori, Z.-X. Shen, T. Kakeshita, H. Eisaki, and S. Uchida, *Phys. Rev. B* **65**, 094504 (2002).
- ⁵⁰S. Sahrakorpi, R. S. Markiewicz, H. Lin, M. Lindroos, X. J. Zhou, T. Yoshida, W. L. Yang, T. Kakeshita, H. Eisaki, S. Uchida, S. Komiya, Y. Ando, F. Zhou, Z. X. Zhao, T. Sasagawa, A. Fujimori, Z. Hussain, Z.-X. Shen, and A. Bansil, *Phys. Rev. B* **78**, 104513 (2008).
- ⁵¹A. Ino, T. Mizokawa, K. Kobayashi, A. Fujimori, T. Sasagawa, T. Kimura, K. Kishio, K. Tamasaku, H. Eisaki, and S. Uchida, *Phys. Rev. Lett.* **81**, 2124 (1998).
- ⁵²B. Barbiellini and T. Jarlborg, *Phys. Rev. Lett.* **101**, 157002 (2008).
- ⁵³G. Sordi, K. Haule, and A.-M. S. Tremblay, *Phys. Rev. B* **84**, 075161 (2011).
- ⁵⁴V. J. Emery and G. Reiter, *Phys. Rev. B* **38**, 4547 (1988).
- ⁵⁵B. Lau, M. Berciu, and G. A. Sawatzky, *Phys. Rev. Lett.* **106**, 036401 (2011); *Phys. Rev. B* **84**, 165102 (2011).
- ⁵⁶J. K. Perry, J. Tahir-Kheli, and W. A. Goddard III, *Phys. Rev. B* **65**, 144501 (2002).
- ⁵⁷E. S. Božin and S. J. L. Billinge, *Phys. Rev. B* **72**, 174427 (2005).